



Geotechnologies Applied to Anthropomorphic Structures: Use of GPR for Detection of Structural Problems, Causes and Effects - Case Study in Coimbra, Portugal

João Duarte^{1*}, José Carvalho²⁾, Joana Ribeiro^{3,4)}

^{1*)} IQGeo - Serviços, Lda e Geosciences Center of the University of Coimbra, Portugal; joao.aduarte@iqgeo.pt; <https://orcid.org/0000-0003-1859-9325>

²⁾ University of Coimbra, Geosciences Center of the University of Coimbra, Portugal; email: jose.carvalho.geo@gmail.com;

³⁾ University of Coimbra, Department of Earth Sciences, Portugal; email: joana.ribeiro@uc.pt; <https://orcid.org/0000-0001-8659-234X>

⁴⁾ Instituto Dom Luiz, Portugal; email: joana.ribeiro@uc.pt; <https://orcid.org/0000-0001-8659-234X>

<http://doi.org/10.29227/IM-2024-01-33>

Submission date: 6.3.2023 | Review date: 27.4.2023

Abstract

One of the recurrent problems in civil construction concerns the wear and deterioration of structures due to their use over time. There should be a plan for monitoring the structures to assess and quantify anomalies, which will allow the minimization and rehabilitation measures to be carried out in advance. This study aimed to use geotechnologies, specifically the Ground Penetrating Radar (GPR), to identify and quantify the damage caused using a swimming pool inserted in a structure built on a residential property. The methodology comprised the use of georadar Sensors & Software PulseEKKO GPR for data acquisition. The data were processed in the software EKKO Project considering the following parameters: 1- Grain/Filter: Dewow + SEC2 Gain (Attenuation:10.00 Start Gain:4.00 Maximum Gain: 950). Seven acquisition profiles were performed: 3 on the East side, 2 on the South side, and 2 on the West side of the pool, with a spacing between 0.8 m. From the visualization of the processed radargrams, and the slices elaborated for each profile with a color palette corresponding to the obtained reflectance values, it was possible to identify the underlying structures of the pavement of the edge of the pool such as beams, beam frames, slope, interior space of the support structure and, most importantly, the degree of subsoil materials alteration, depth, and dispersion of water infiltrations. On the East side, the pool is inserted into the rock formation; it is possible to identify up to 1 m depth of the water infiltration and dispersion. To the West and South, the pool is supported by a built-up structure; underneath there is a hall and the engine room. In these places, the infiltration and dispersion of water were identified until approximately 0.7 m depth, as well as the existing structures and their condition. The 0.7 m corresponds to the thickness of the existing slab and beams. Based on these results, an intervention plan was prepared for the rehabilitation of the deterioration of the materials and the minimization of water percolation through the waterproofing of the pool's surrounding areas.

Keywords: ground penetrating radar, geotechnologies, monitoring of anthropomorphic structures, detection of structural problems

Introduction

The use of non-destructive techniques for monitoring and assessing the condition of man-made structures has been one of the goals of modern science. These techniques, such as Ground Penetrating Radar (GPR), electrical resistivity, and electromagnetic induction, allow for characterizing, locating, and modelling 2 and 3D of anthropic structures, as well as characterizing the locations of their implantation [1, 2]. It is recurrent to identify wear and tear and deterioration marks in structures due to their use and the passage of time. The ideal would be to have a plan for monitoring the systems to evaluate and quantify the anomalies detected, which would allow the minimization and rehabilitation of the detected evidence [3-6].

In this case study the geophysical method used was the GPR [7, 8] because it presents clear advantages to other methods. Its use in anthropic and geological structures [9] is known for its resolution, easy handling, immediate visualization of the collected data and reduced spaces. In this case study the geophysical method used was the GPR [7],[8] because it presents clear advantages to other methods. Its use in anthropic and geological structures [9] is known for its resolution, ease of handling, immediate visualization of the collected data and reduced spaces.

Location and Geology

This study was carried out in central Portugal, in the city of Coimbra, integrated into urban development at the location indicated in figure 1. The implantation of the structure is in the bedrock belonging to the Grés de Silves Formation [10].

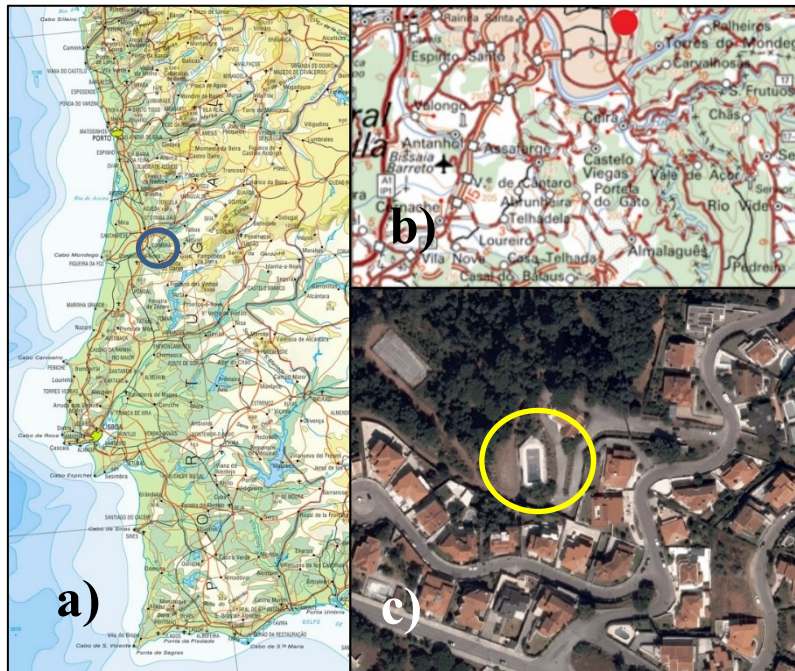


Fig. 1. a) Blue circle - Location of Coimbra on the Portugal map. b) Red circle - Location on map excerpt (Military map of Portugal 1:25 000. Continent, series M888; 241 - Coimbra (South)) - Accessed 14/02/2023. c) Yellow circle - Pool location in Google Earth Image - Accessed 14/02/2023.

Method and Methodology

Ground Penetrating Radar survey

The GPR method is an active EM geophysical method for the acquisition and recording of in-depth information from the subsurface. It works by sending a small electromagnetic energy impulse in depth along the subsurface, with a certain frequency, from a transmitting antenna (TX), and records the intensity and time of the return of that same impulse that reaches the receiving antenna (RX) [8,11]. After penetrating underground and along their path between the TX and RX antenna, electromagnetic impulses undergo phenomena of reflection, refraction, attenuation, and absorption, which are intrinsically linked to the properties of electrical conductivity, dielectric permittiveness and magnetic permeability of materials traversed by that same wave/impulse EM.

Thus, the time of sending and returning a signal in depth (velocity of wave propagation in the middle) indicates the apparent depth to which a given target/discontinuity is found between materials; the contrast in the amplitude/intensity and aspect of the reflection of that signal at that point indicates the differences between the dielectric properties between these material means, structures and objects (the greater the contrast between them, the greater the amount of electromagnetic energy reflected in this point).

This procedure is carried out along acquisition profiles/lines, whereby the data received by the receiving antenna is transferred to a computer so that it can be digitized and recorded as 2D sequences of individual traces, called radargrams. Interpretation may be performed from the "raw" radargrams and/or after applying various visualization and/or processing techniques.

Finally, a sequence of 2D profiles can be interpolated into the SliceView module of the EKKO_Project™ software which was used to process the data and create a series of amplitude slices at various depths. These "time slices" represent planar images at a given depth where the different "anomalies" (evident contrasts in the reflective properties of the materials) are visualized and interpreted, which should correspond to the structures present in the investigated environment.

To perform this work, the geophysical method used was the GPR, and the data acquisition was done using the SENSORS & SOFTWARE PULSEKKO GPR equipment (Figure 2), configured according to the parameters presented in table 1.



Fig. 2. SENSORS & SOFTWARE PULSEKKO GPR equipment.

Tab. 1. Equipment Configuration Parameters

Data Collected	2023-Jan-13
Survey Type	Reflection
Acquisition mode and trigger	Continuous, odometer
Antenna type	Bi-static, shielded
Frequency (Mhz)	500.00
Time Window (ns)	100.00
Speed of the environment	0.100 m/ns
Step Size (m)	0.020
Antenna Separation (m)	0.23
Dynamic Stacking (medium value)	16
Maximum depth of investigation (m)	±4,50

The software EKKO Project was used for data processing, considering the following parameters: 1- Grain/Filter: Dewow + SEC2 Gain (Attenuation:10.00 Start Gain:4.00 Maximum Gain: 950). Methodologically, it was chosen to perform a line acquisition, according to the locations and orientations indicated in figure 3 (yellow arrow indicates the beginning and direction of the acquisition). Seven acquisition profiles were performed: 3 on the East side, 2 on the South side, and 2 on the west side of the pool, with a spacing between 0.8 m, and with the direction indicated in figure 3.

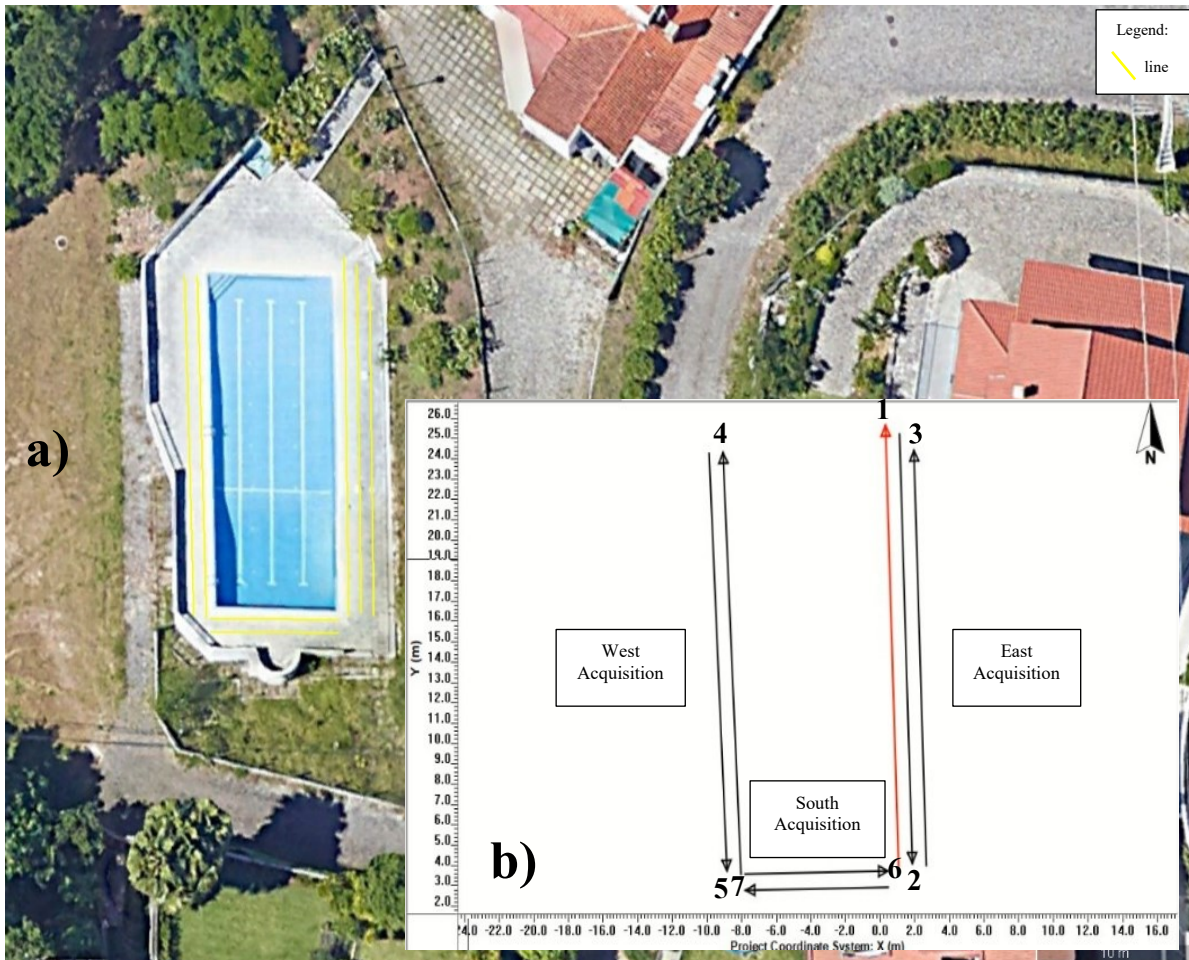


Fig. 3. (a) – Location (Yellow lines). (b) – Orientation, and direction of GPR profiles.

Results And Discussions

After processing the original data and radargrams (Figures 4 and 5), radargrams were obtained and slices per profile were extracted with a colour palette corresponding to the reflectance values, which enables better identification of the underlying structures of the pool edge pavement. Such as the beams, slope, beam frames, interior space of the support structure and most importantly the degree of alteration of the materials, depth, and dispersion of the water infiltrations.

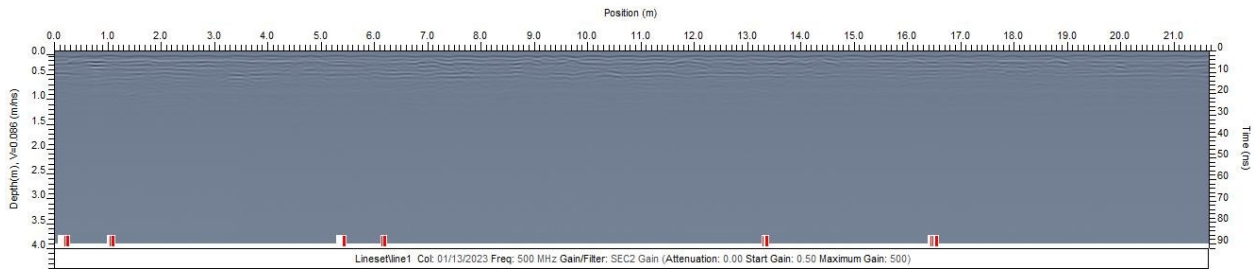


Fig. 4. Radargram Lineset 1. East acquisition. No processing.

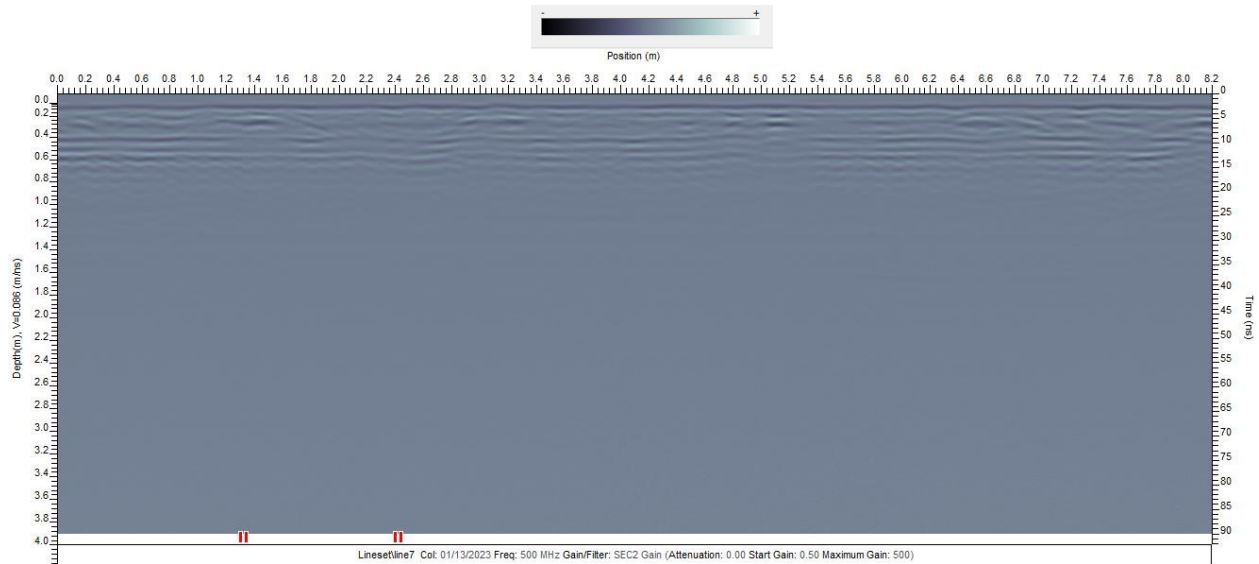


Fig. 5. Radargram LineSet 7. South Acquisition. No processing.

In the following figures, the radargrams are shown after processing. The information on the radargrams shown in figures 4 and 5 can be compared with the corresponding radargrams in figures 6 and 12.

The results obtained from the acquisition performed on the East side (Lines 1, 2 and 3), show that on the surface, as expected, no significant changes were identified, and it is possible to see the floor slabs (blue polygon). At a depth of 0.50-0.55 m, marked by the red polygon, it is possible to identify the beam and the reinforcements, as well as the stratified area (white polygon). It is also possible to identify what appears to be a box and pipes (yellow and green circles). From 1.1-1.15 m depth, for the radargrams of lines 1, 2 and 3, the signal is different, partly due to the rocky substrate in which the structure is set (grey dashed line). There is also a lot of noise below this depth from signal attenuation due to the materials above (rock with high content of iron and clay and seepage water). All this structure is visible on the remaining processed radargrams (Figures 6, 7 and 8).

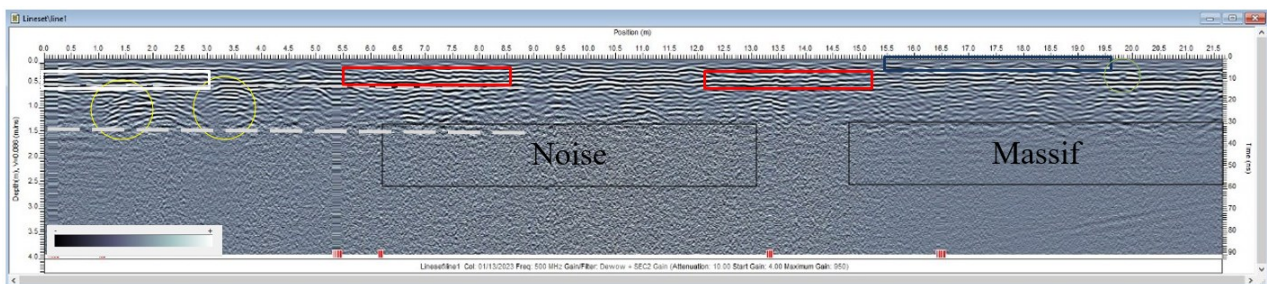


Fig. 6. Radargram Lineset 1. East acquisition. Processed.

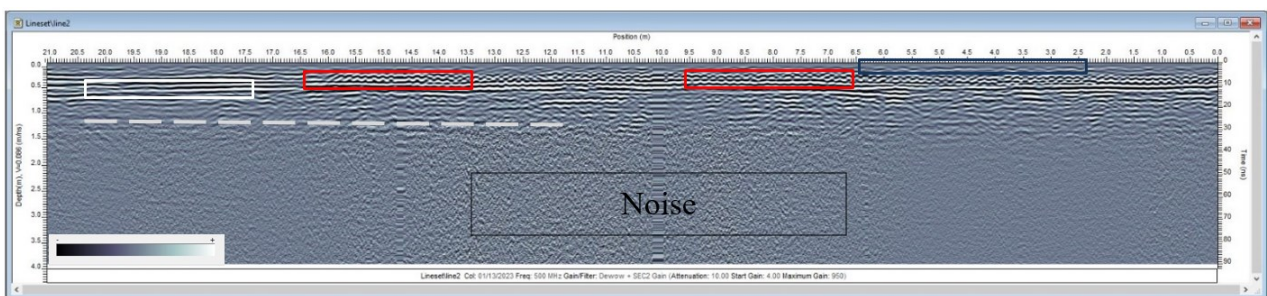


Fig. 7. Radargram Lineset 2. East acquisition. Processed.

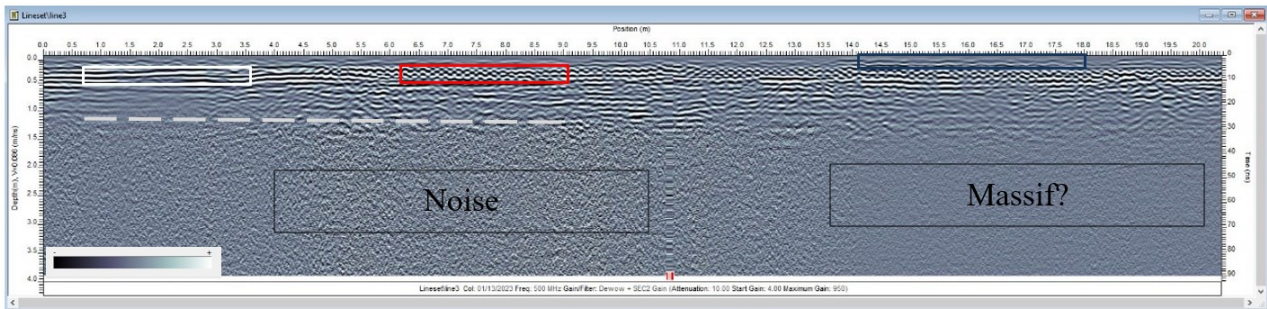


Fig. 8. Radargram *Lineset 3*. East acquisition. Processed.

On the West side (Lines 4 and 5), it can also be seen that on the surface, no significant alterations are observed, and it is possible to see the floor slabs (blue polygon). At a depth of 0.50-0.55 m, marked by the red polygon, it is possible to identify the beam and the frames, as well as the stratified area (white polygon). It is also possible to identify what appears to be a box and pipes (yellow and green circles). From 1.5-1.7 m depth, for the radargrams of lines 4 and 5, the signal is different and is partially attenuated by the materials above (iron and seepage water) and by the existing void resulting from the built structure (Figure 11) (grey dashed line). All these structures are visible on the remaining processed radargrams (Figures 9 and 10).

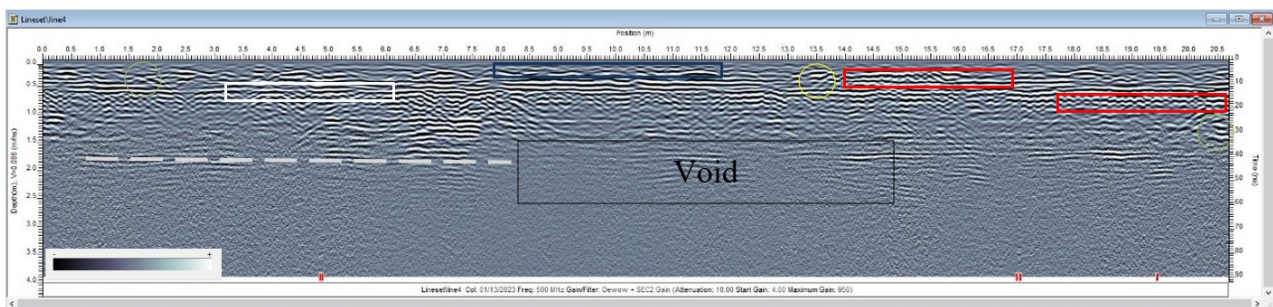


Fig. 9. Radargram *Lineset 4*. South acquisition. Processed.

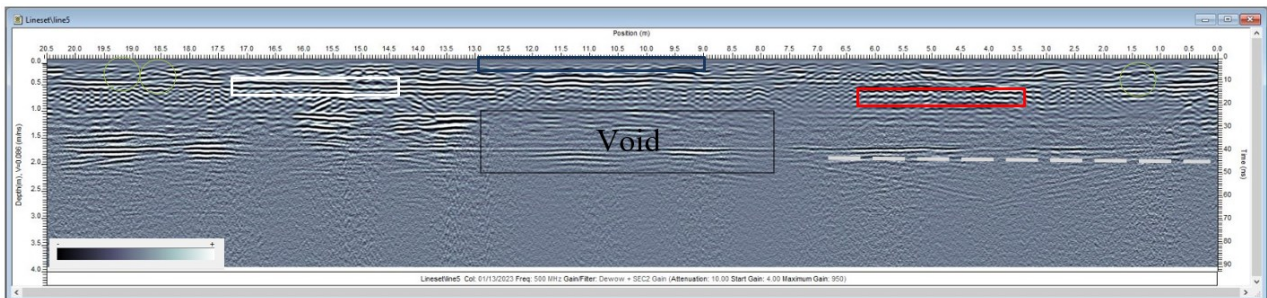


Fig. 10. Radargram *Lineset 5*. South acquisition. Processed.



Fig. 11. Interior and exterior of the structure correspondent lines 4 and 5.

On the South side (Lines 6 and 7), it is also possible to see no significant changes on the surface, with the floor slabs being visible (blue polygon). At a depth of 0.60-0.70 m, marked by the red polygon, it is possible to identify the beam and the frames. It is also possible to identify what appears to be piped (green circle). From 1.5-1.7 m depth, for the radargrams of lines 6 and 7, the signal is different and is partially attenuated by the materials above (iron, rock with high iron and clay contents and infiltration water) and by the existing void resulting from the built structure (grey dashed line). All these structures are visible on the remaining processed radargrams (Figures 12 and 13).

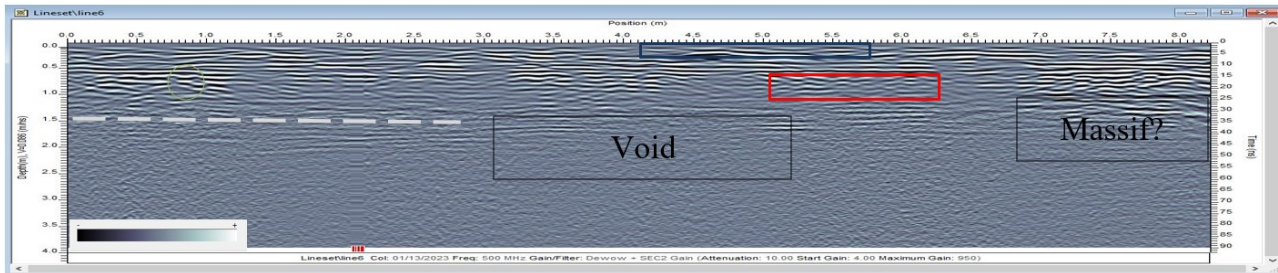


Fig. 12. Radargram *Lineset 6*. West acquisition. Processed.

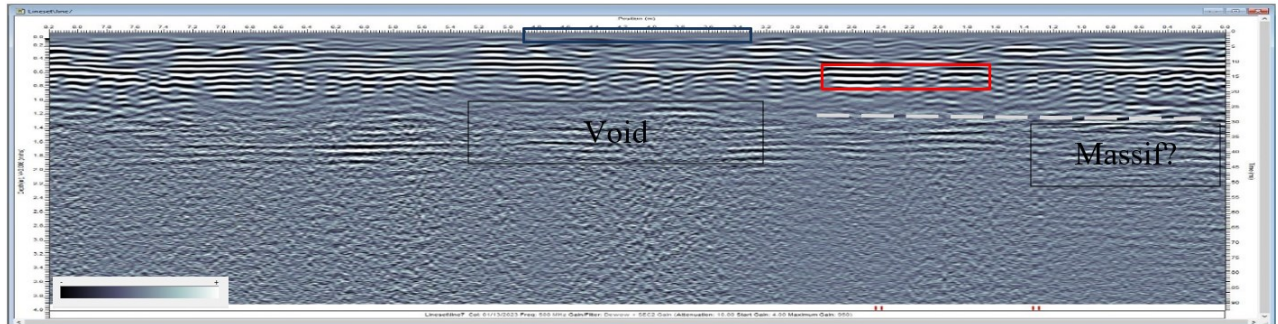


Fig. 13. Radargram *Lineset 7*. West acquisition. Processed.

After processing, the software assigns a colour palette to the reflectance values, creating a series of amplitude slices at various depths with the variations existing in the area studied. Figure 14 shows these variations at defined depths, which gives an insight into their development and distribution. Six slices were selected with depths ranging from the surface to 1.7 m.

At the surface, as it had been referred from the visualisation of the radargrams, there are no significant changes mirrored in the uniformity of the reflectance values. In this case, the surface was dry and structurally sound.

At 0.35-0.40 m depth, corresponding to the slab, there are some significant changes with high reflectance values on the East side, possibly corresponding to water infiltration in the rock mass and on the west side to water infiltration in the contact between the pool and the slab, at the point where there are higher reflectance values. At a depth of 0.50-0.55 m, the alteration in the structure is notorious. By water infiltration and the presence of iron from the beams of the structure. As can be seen in figure 11, the frames are bare and with high rates of deterioration. From 0.65-0.70 to 1.65-1.70 m depth, the variations in reflectance values tend towards uniformity and lower values. This fact is because underneath the deteriorated structure there is an open space which corresponds to the interior storage space of equipment and machinery related to the swimming pool maintenance (Figure 11). In the last slice, it is possible to identify a change in the southwest corner, which will correspond to an occurrence in the masonry wall built in the structure, as can be seen in the last photograph of Figure 11.

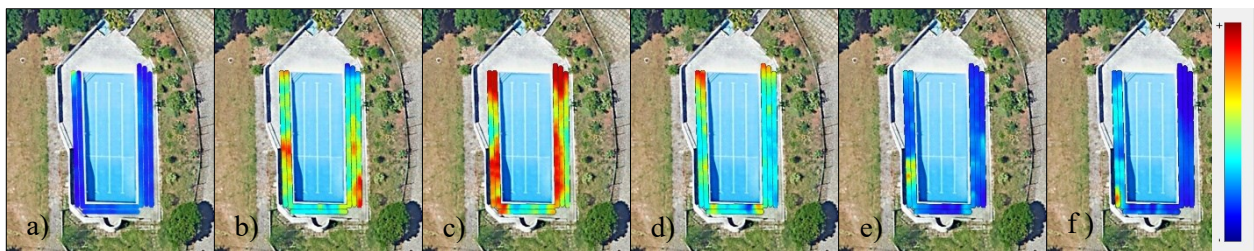


Fig. 14. a) Surface Slice. b) Slice to a depth of 0.35-0.40 meters. c) Slice to a depth of 0.50-0.55 meters. d) Slice to a depth of 0.65-0.70 meters. e) Slice to a depth of 1.10-1.15 meters. f) Slice to a depth of 1.65-1.70 meters.

Conclusions

The GPR method proved to be versatile, without the need for major preparations of the acquisition site, easily allowing to vary the acquisition parameters in an expeditious way and visualise in real-time the acquisition result. Its use allowed the identification of significant anomalies at the marked locations, with significant variations in the reflectance values of the materials, which may be related to the passage of water in some locations due to poor waterproofing, being the probable cause of the damage verified in the building. It is also verified that the location and variation of high reflectance values are always from the edge of the pool to the outside and up to a depth of 0.55 m, which by on-site observation corresponds to the location of the structures. The proposed methodology and method proved to be effective in identifying the patterns of anomalies and structures existing in the studied site and should be used in more and other situations of analysis, to validate them as a non-invasive process, with potential for location, quantification, and dispersion of anomalies.

In the future it will be important to make a data acquisition that allows 2D and 3D modelling of the study site, aiming the visualization and the horizontal and vertical determination, as well as the correlation of the mentioned elements.

Acknowledgments

Our thanks to IQGeo-Serviços, to the Earth Sciences Department of the University of Coimbra and to the engineer Ana Laura Pinto for the opportunity and conditions made available for the realization of this work. The Centro de Geociências (Geosciences Centre) is funded by the Portuguese State through the FCT - Fundação para a Ciência e a Tecnologia (Foundation for Science and Technology) within the scope of the strategic project UIDB/00073/2020 and UIDP/00073/2020.

References

1. Annan, A. P.; Cosway, S. W., 'Ground penetrating radar survey design', in 5th EEGS Symposium on the Application of Geophysics to Engineering and Environmental Problems, SAGEE'92, Oak Brook (1992) 329-352, <https://doi.org/10.4133/1.2921946.36>.
2. Annan, A. P. (2003). Ground penetrating radar - Principles, procedures & applications. Sensors & Software Inc. Canada. 271 pp.
3. Azerêdo, A. C. (2007). Formalização da litoestratigrafia do Jurássico Inferior e Médio do Maciço Calcário Estremenho (Bacia Lusitânica). *Comunicações Geológicas*, 94, 29-51.
4. Barraca, N., Matias, M., & Almeida, F. (2019). O método de radar de penetração no solo (GPR) na caracterização do Mosteiro da Batalha. *Conservar Património*, 32.
5. Barraca, N.; Almeida, M.; Varum, H.; Matias, M. S. (2014). 'The use of GPR in the rehabilitation of built heritage', in *Near Surface Geoscience 2014 - 20th European Meeting of Environmental and Engineering Geophysics*, Athens. <https://doi.org/10.3997/2214-4609.20141998>.
6. Carvalho, J. L. L. (2018). Casos de estudo com utilização de GPR-Reconhecimento e caracterização de estruturas geológicas, arqueológicas e estruturas subterrâneas (Master dissertation, Universidade de Coimbra).
7. Duarte, J., Pedrosa, D., Carvalho, J., Figueiredo, F., & Catarino, L. (2019). Use of Non-Destructive Methods in Structural Analysis of Petrous Materials-Ultrasonic Testing and Ground Penetrating Radar (GPR). In *IOP Conference Series: Earth and Environmental Science* (Vol. 221, No. 1, p. 012061). IOP Publishing.
8. Duarte, J., Carvalho, J., & Figueiredo, F. (2019). Use of Ground Penetration Radar (GPR) in the Evaluation of Geological-Structural Elements of Ornamental Carbonated Rocks-Case Study in Valinho De Fatima, Portugal. In *IOP Conference Series: Earth and Environmental Science* (Vol. 362, No. 1, p. 012101). IOP Publishing.
9. H. M. Jol (2009). *Ground penetrating radar: Theory and applications*. 1st edition. Elsevier Science.
10. Lai, W. W. L.; Dérobert, X.; Annan, P. (2017). 'A review of ground penetrating radar application in civil engineering: A 30-year journey from locating and testing to imaging and diagnosis', *NDT & E International* 96. 58-78, <https://doi.org/10.1016/j.ndteint.2017.04.002>
11. Tareco, H.; Grangeia, C.; Varum, H.; Matias, M. S. (2009). 'A high resolution GPR experiment to characterize the internal structure of a damaged adobe wall', *First Break*, 27(8), 79-84. M. P. Brown and K. Austin, *The New Physique* (Publisher Name, Publisher City, 2005), pp. 25-30.